

Paraelectric resonance study of $\text{KCl}:\text{}^7\text{Li}^+$

F. Holuj

Department of Physics, University of Windsor, Windsor, Ontario Canada N9B 3P4

Frank Bridges

Board of Studies in Physics, University of California, Santa Cruz, California 95064

(Received 24 September 1982)

A paraelectric resonance study has been made of $\text{KCl}:\text{}^7\text{Li}^+$ over the frequency range 20–150 GHz. The data have been fitted to a $\langle 111 \rangle$ -dipole model. The best-fit tunneling parameters (including the estimated systematic errors) are $\eta = -11.34 \pm 0.4$, $\mu = -3.55 \pm 0.4$, and $\nu = 0.21 \pm 0.4$. The electric dipole moment is 5.683 ± 0.06 D. These parameters are compared critically with the existing data on $\text{KCl}:\text{}^7\text{Li}^+$.

I. INTRODUCTION

$\text{KCl}:\text{}^7\text{Li}^+$ is perhaps the best known paraelectric-paraelastic system and has been studied extensively. There are several papers whose subject was the paraelectric resonance (PER) in this substance,^{1–5} which includes studies when the crystal was subjected to stress.^{4,5} Additionally, the $\text{KCl}:\text{}^7\text{Li}^+$ tunneling multiplet was used to generate phonons at microwave frequencies.^{6–8} Yet the estimate of the tunneling parameters of this system is based on the PER performed at a few frequencies in the range of 10–70 GHz. In the following we present the results of the PER study of $\text{KCl}:\text{}^7\text{Li}^+$ crystal extended to 150 GHz.

The paraelectric nature of this crystal arises from the fact that Li^+ occupies an off-center position of the K^+ vacancy. It is widely believed that this displacement creates an electric dipole along a $\langle 111 \rangle$ direction of KCl. Symmetry arguments demand that there be eight such directed dipole states. These in turn form the tunneling multiplet which can be studied, usually at low temperatures. Early studies showed that the off-center model is feasible and recent studies have used improved potentials to discuss the behavior of Li^+ in alkali halides.^{9,10}

The PER method affords perhaps the most direct way to study the paraelectric-paraelastic systems. Experimental data yield the tunneling parameters (called η , μ , and ν) which determine the “zero-field” splitting (ZFS) of the multiplet and, most importantly, the electric dipole moment p . These usually permit an unambiguous assignment of the model describing the paraelectric system.

II. THEORETICAL BACKGROUND

We shall adopt the “tunneling model,” which treats the lowest multiplet of energy levels as isolated, ignoring thereby all other excited multiplet

states. The tunneling model is best described using the directed basis states which are the eigenstates in the presence of large electric fields. Each state represents the dipole oriented along one of a set of equivalent axes within the crystal. All other dipole orientations are not permitted and, therefore, the dipole energies in the presence of an electric field will be “quantized.” To restrict the dipole orientation to a few directions, a multiwell potential is assumed which has minima lying along the above-mentioned equivalent symmetry axes. The eigenstates of the system then correspond to the dipole moment occupying one or more of these potential wells. The symmetry of this potential must be consistent with the symmetry of the host lattice, and, therefore, in the present case must have the O_h symmetry of the cubic KCl host. The three simplest models for cubic crystals are the following: the $\langle 100 \rangle$ model with six minima along the $\langle 100 \rangle$ axes; the $\langle 111 \rangle$ model with eight minima along the $\langle 111 \rangle$ axes; the $\langle 110 \rangle$ model with 12 minima along the $\langle 110 \rangle$ axes. The model which we adopt for Li^+ is $\langle 111 \rangle$. Its directed dipole states are indicated in Fig. 1.

The theory describing this model is well known.¹¹

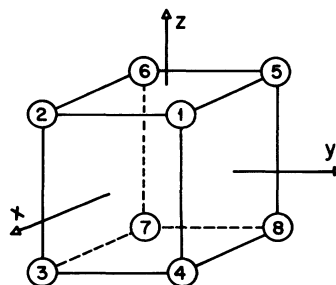


FIG. 1. Directed state labeling for the $\langle 111 \rangle$ -dipole model of $\text{KCl}:\text{}^7\text{Li}$. The dipoles are assumed to point towards one of the numbered open circles.

Here we shall limit ourselves to the following. The tunneling parameters are defined as

$$\begin{aligned}\eta(70.5^\circ) &= \langle 1 | H_c | 2 \rangle = \langle 1 | H_c | 5 \rangle = \cdots, \\ \mu(109.5^\circ) &= \langle 1 | H_c | 3 \rangle = \langle 1 | H_c | 6 \rangle = \cdots, \\ \nu(180^\circ) &= \langle 1 | H_c | 7 \rangle = \langle 2 | H_c | 8 \rangle = \cdots,\end{aligned}\quad (1)$$

where $\langle i | H_c | j \rangle$ is the matrix element of the crystal field H_c between the directed states i, j and 70.5° is the reorientation of the dipole between these states, etc. The theoretical ZFS is

$$\begin{aligned}E(A_{1g}) &= 3\eta + 3\mu + \nu, & E(T_{1u}) &= \eta - \mu - \nu, \\ E(T_{2g}) &= -\eta - \mu + \nu, & E(A_{2u}) &= -3\eta + 3\mu - \nu.\end{aligned}\quad (2)$$

The differences between the neighboring levels are

$$\begin{aligned}E(T_{1u}) - E(A_{1g}) &= -2\eta - 4\mu - 2\nu, \\ E(T_{2g}) - E(T_{1u}) &= -2\eta + 2\nu, \\ E(A_{2u}) - E(T_{2g}) &= -2\eta + 4\mu - 2\nu.\end{aligned}\quad (3)$$

Finally, the interaction of the electric dipole moment with the dc electric field applied externally is

$$H_E = -\vec{p} \cdot \vec{E}. \quad (4)$$

The diagonal terms which Eq. (4) introduce are tabulated in Ref. 11.

III. APPARATUS AND EXPERIMENTAL PROCEDURE

The microwave spectrometer and the associated electronics used in this research have been described elsewhere.¹² The cavity has also been described.¹³

The crystal samples were prepared from a single-crystal boule grown at the Crystal Growth Laboratory of the University of Utah, Salt Lake City, and doped in the melt with LiCl. The melt molar concentration of ${}^7\text{Li}$ was $2 \times 10^{-4} M$.

The crystal wafers were cut from the boule with a wet string saw and were first oriented along one of the (100), (111), or (110) planes using an especially constructed jig as the holder in the x-ray diffractometer. They were then lapped on a damp cloth so that the finished wafer was accurately oriented along the chosen plane. The accuracy of this orientation is estimated to be within 0.5° . We rarely used the crystal samples more than twice. We thereby avoided the degradation of the spectrum which sets in when the crystal is strained by frequent handling. This was done especially after the crystal had been immersed in excessive electric fields. A Mylar sheet was used in some runs to prevent the electrical breakdown. In these cases the dc electric field was calculated from

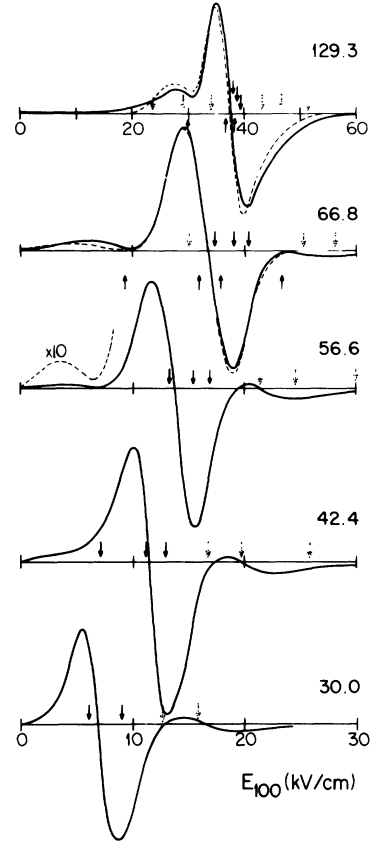


FIG. 2. Trace recording of PER spectrum for E_{100} . Downward-pointing arrows indicate theoretical resonant E fields as obtained from Fig. 4. Solid and dotted arrows represent, respectively, the allowed and forbidden transitions. Upward-pointing arrows in the two topmost traces indicate the centers of the Gaussians (shown as dashed lines). All were obtained at 4.2 K. The frequencies are given in GHz.

$$E_{dc} = V / (l_x - l_m \epsilon_x / \epsilon_m), \quad (5)$$

where V is the applied voltage, and l_x and l_m are the thicknesses of the sample and the Mylar sheet, respectively (as measured with a dial gauge). The corresponding dielectric constants are $\epsilon_x = 5.03$ (Ref. 14) and $\epsilon_m = 3.0$.¹⁵ In all cases described here \vec{E}_{dc} was parallel to the microwave \vec{E} vector. Most experiments described here were performed at 4.2 K, although some were also checked at 1.5 K.

IV. RESULTS

In Figs. 2 and 3 we present some trace recordings of the PER resonances for the applied electric field along the [100], [111], and [110] directions. (We shall designate these field orientations as E_{100} , E_{111} , and E_{110} , respectively.) Figure 2 shows five record-

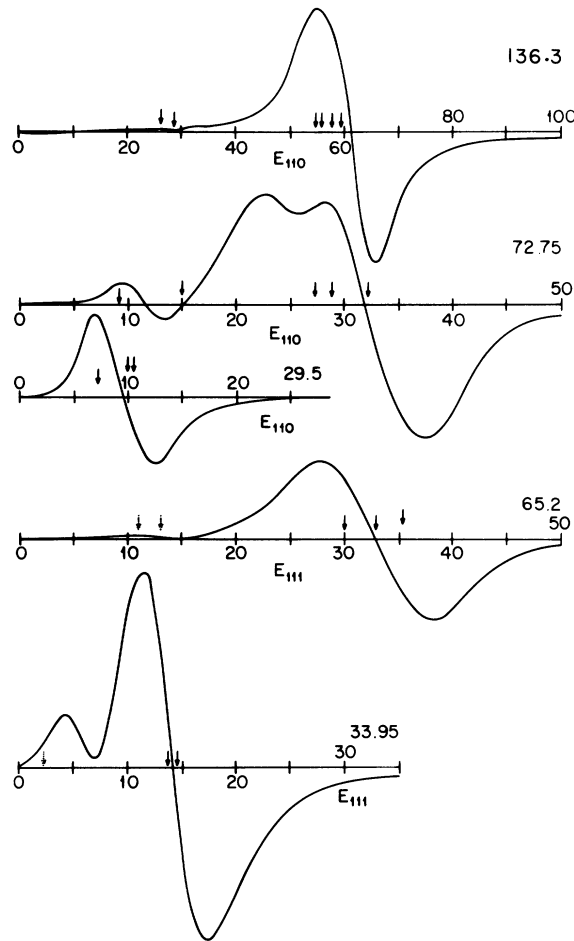


FIG. 3. Trace recording of PER spectrum for E_{110} (kV/cm) and E_{111} (kV/cm) of $\text{KCl}:\text{}^7\text{Li}$. See Fig. 2.

ings for PER signals for E_{100} . Those obtained at 129.3 and 66.8 GHz also include Gaussian derivative curves (whose centers are indicated by upward-pointing arrows) which best approximate the experimental signals. They illustrate the fact that the PER signals cannot be approximated by a single or multiple Gaussian curves. The recordings for E_{110} and E_{111} are shown in Fig. 3. The sample thickness for E_{111} was 1.24 mm and for E_{110} was 0.50 mm. Here again the signals are complex and, moreover, are broader than for E_{100} . In Figs. 2 and 3 the solid and dotted downward-pointing arrows indicate the positions of the allowed and forbidden transitions, respectively, as predicted by theory.

The resonant electric fields were estimated from the trace recordings such as those shown in Figs. 2 and 3. Table I lists the numerical data which apply to these recordings. We have listed E_{ijk} (whose significance was explained above), the experimental resonant frequency (column 2), the resonant electric

field (column 5), and ω_k which assigns a "confidence index" for the k th line of the given PER spectrum ($\omega_k = 1$ to 3 according to the confidence index which included the ease of measurement).

A total of over 100 traces each with several resonances were obtained for the three crystal orientations using a variety of sample thicknesses from 0.5 to 1.3 mm. The positions (in kV) of these lines as a function of frequency are plotted in Figs. 4–6. The most intense resonances ($\omega_k = 2$ or 3) are plotted as open circles and the broad "satellites" flanking the main resonance are plotted as open squares. Figures 4, 5, and 6 are for E_{100} , E_{111} , and E_{110} , respectively. Qualitatively, the resonances obtained by us are similar in every respect to those published previously.^{1–3} For comparison, we have included a few data points from earlier investigations. Diamonds in Figs. 4 and 6 present data from Ref. 1, the open triangles present data from Refs. 2 and 5, and solid triangles present data from Ref. 3. These entries must be treated as approximate, since they were read off the published diagram.

Some 260 of the experimental resonant electric fields were used in a computer program whose aim was to estimate the tunneling parameters p , η , μ , and ν for the tunneling model $\langle 111 \rangle$ (Fig. 7). The basis of the program was a modified version of the Newton-Raphson method. The method can be described as follows¹⁶: Let $f(P)$ be the sum of squares

$$f(P) = \sum_k \left[\frac{(E_{k_1} - E_{k_2}) - E_k}{n} \right]_{\omega_k}^2, \quad (6)$$

where $(E_{k_1} - E_{k_2})$ is the calculated transition frequency and $n = m - s$ is the number of degrees of freedom (m is the number of transitions measured; s is the number of parameters); E_k is the experimental resonant frequency. The calculated energy levels E_{k_i} are functions of parameters $(P_1, P_2, \dots) = \vec{P}$ whose values are to be determined by the condition that $f(\vec{P})$ is a minimum:

$$(\partial/\partial P_i) f(\vec{P}) = 0. \quad (7)$$

The probable error was calculated as follows. The least-square sum f may be in error due to statistical variations in the measurements by an amount $\Delta f \simeq f/n$. The corresponding error σ_i in the optimized parameter P_i is obtained from the equation

$$\Delta f = \frac{1}{2} \sum_{i,j} M_{ij} \sigma_i \sigma_j \simeq f/n, \quad (8)$$

where

$$M_{ij} = \frac{\partial^2 f}{\partial P_i \partial P_j}. \quad (9)$$

TABLE I. Experimental data for Figs. 2 and 3. "Transitions" are also indicated in Figs. 4–6. See text for the meaning of "weight." The choice of data for this table and Figs. 2 and 3 is arbitrary.

Orientation	Frequency (GHz)	Transitions	Weight	Field kV/cm
E_{100}	30.0	2-4,3-5	1	15.5
		2-5	3	6.5
	42.4	2-4,3-5	2	19.0
		2-5	3	11.5
	56.6	2-4,3-5	1	21.5
		2-5	3	14.5
	66.8	2-6,1-5	1	5.8
		2-4,3-5	1	24
		1-4	3	17
		2-6,1-5	1	9.5
129.3	2-4,3-5	1	42.5	
	1-4	3	37.5	
	2-6,1-5	1	32.0	
E_{111}	33.95	(3,4)-(6,7),5-8,2-5	3	14.0
	65.2	(3,4)-(6,7),1-2,2-5	2	5.7
E_{110}	29.5	2-8	2	12.5
		3-7,2-5,5,8	2	9.0
	72.75	2-5	3	32.0
		3-7	2	26.5
	136.3	2-8,1-7	1	11.5
	2-5	3	61.5	
	2-8,1-7	1	28.13	

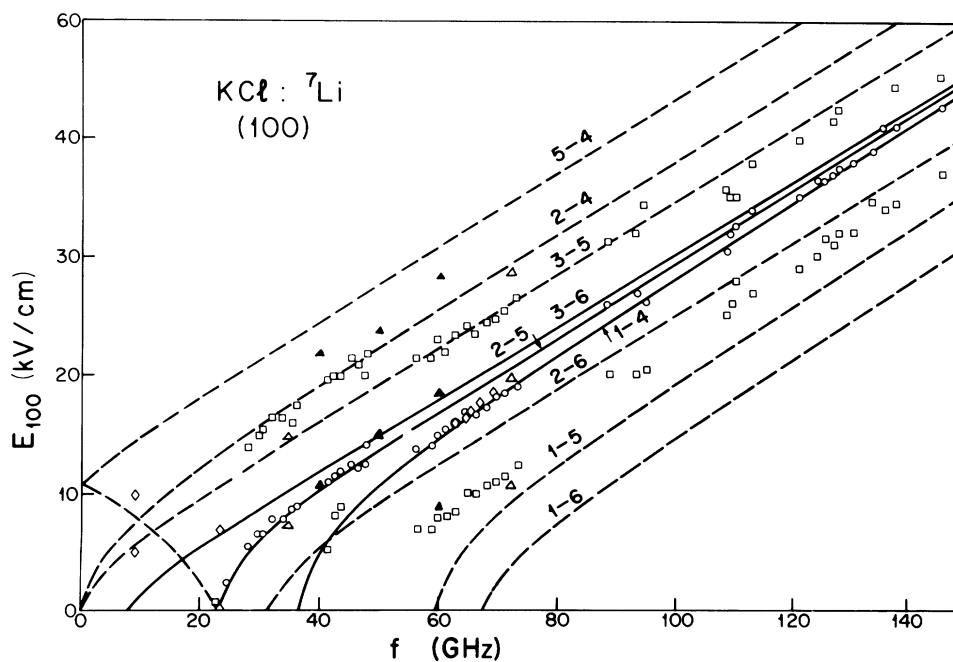
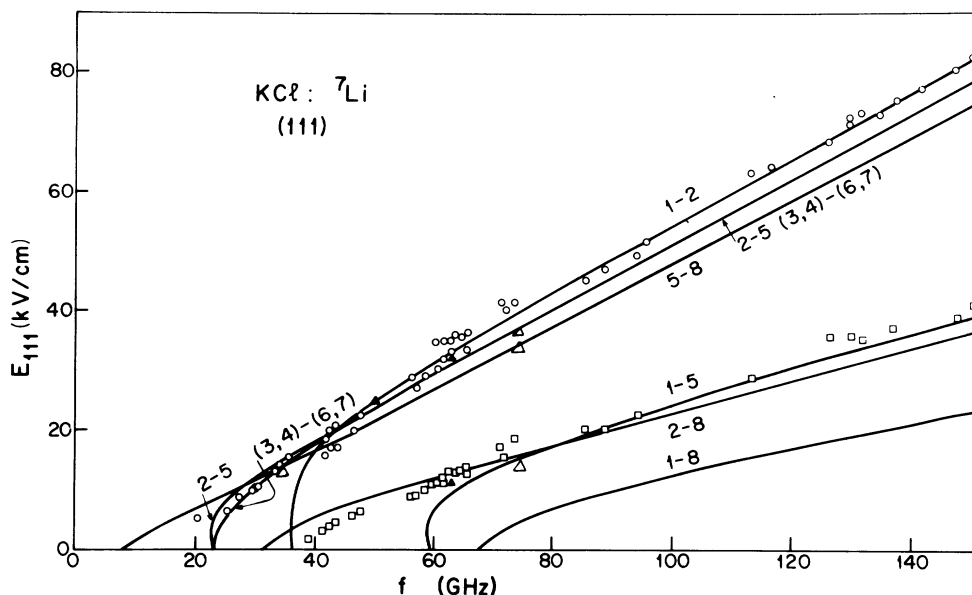


FIG. 4. Plots of resonant frequency f vs the electric field E_{100} . Experimental values are represented by points and the predicted values by curves. Open circles (and solid lines) are allowed resonances, squares (and dashed lines) are forbidden resonances. Triangles and diamonds are resonances obtained from other publications as explained in the text.

FIG. 5. Plot for E_{111} . See Fig. 4.

Inversion of (8) gives, for the mean-square error in P_i ,

$$\sigma_i^2 = 2M_{ii}^{-1}(f/n). \quad (10)$$

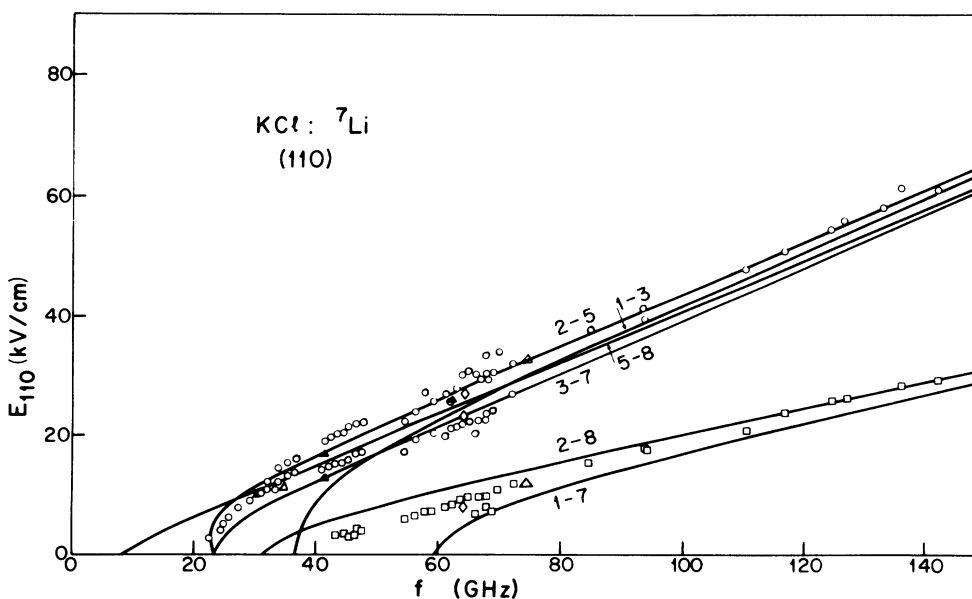
The probability of the electric dipole transition for levels $i \rightarrow j$ was also calculated using the formula

$$I = (n_i - n_j) | \langle i | \vec{E}_{rf} \cdot \vec{p} | j \rangle |^2, \quad (11)$$

where n_i is the normalized population of the i th level (a function of T) and \vec{E}_{rf} is the microwave electric

field which was assumed to be parallel to \vec{E}_{dc} . \vec{p} was assumed to be equal to its value in Table III, and the amplitude of E_{rf} was normalized to unity. I was calculated for each transition, and if it was smaller than 10^{-5} (an arbitrary limit), the transition was considered "forbidden" and rejected by the program.

In our analysis we first matched the dominant experimental line to the strongest theoretical line at each frequency. In cases where other allowed transi-

FIG. 6. Plot for E_{110} . See Fig. 4.

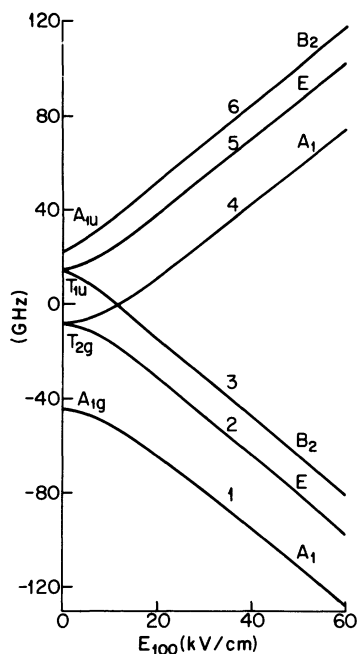


FIG. 7. Energy levels of the tunneling multiplet for E_{100} . The labels are the irreducible representations of O_h and C_{4v} point groups.

tions were close together (within 5 GHz) and a composite allowed spectra expected, a weighted average was matched to the data.

Figure 4 shows one peculiarity: an apparent jump

of the line positions between 45 and 55 GHz. It was repeatedly examined on several samples of different thicknesses. It can be explained as follows. At frequencies below 45 GHz by virtue of its narrow linewidth and intensity the line 2-5 is dominant. The line 1-4, although very intense, is either too broad to be seen (just above 35 GHz) or had not yet appeared (just below 35 GHz). At frequencies above 55 GHz, however, the transition 1-4 had become sufficiently narrow to be dominant. (The reason why the width of the 1-4 transition is expected to be variable in this region is, of course, connected with the rapid variation of its slope, as is evident in Fig. 4.) Table II is an aid to this discussion. It contains the relative intensities of the allowed lines, displayed also in Figs. 2 and 3. Using this table and Figs. 4-6 we conclude that the experimental points do indeed fit the most intense transitions well.

Returning to the above-mentioned jump in Fig. 4 we note that the weak satellite line at high E_{100} fields is very broad and difficult to locate; Fig. 3 gives several examples of this. Below approximately 45 GHz it is somewhat better resolved than above approximately 55 GHz at which region it is almost impossible to locate reliably. In the light of the previous discussion it is obvious why this line is expected also to undergo an apparent jump between 45 and 55 GHz: Below 45 GHz the dominant line 2-5, which is narrow and of medium intensity, overlaps the satellite less than the broad and intense line 1-4

TABLE II. Relative transition probabilities (in GHz) of a selected set of traces. Those also shown in Figs. 2 and 3 are marked by an asterisk.

E_{100}	Transition	130*	67*	42*	30*
	1-4	1	1	1	
	2-5	0.559	0.559	0.545	1
	3-6	0.029	0.020	0.027	0.047
E_{111}	Transition	120	65*	42	34*
	1-2	1	1	1	1
	2-5	0.283	0.422	0.417	0.357
	(3,4)-(6,7)	0.136	0.220	0.250	0.230
	5-8	0.049	0.115	0.121	0.106
	1-5	0.223	0.168		
	2-8	0.111	0.136	0.128	0.089
	1-8	0.004	0.0004		
E_{110}	Transition	136*	73*	42	30*
	2-5	0.206	0.207	0.200	0.647
	1-3	1	1	1	
	5-8	0.039	0.067	0.067	0.184
	3-7	0.193	0.337	0.337	1
	2-8	0.064	0.071	0.067	
	1-7	0.073	0.060		

TABLE III. A comparison of the values of tunneling parameters published previously with those found in this work. The fifth row contains the relative rms errors and the systematic errors (the larger of the two).

Ref.	p	η	μ	ν	Frequencies (GHz)	Experimental ZFS (GHz)
1	5.6 ± 0.2	-11.55 ± 0.9	0	0	63,24,9	23.1 \pm 1.0, 32.1 \pm 1.2
2	6.3 ± 0.3	-11.3 ± 0.2	-3.2 ± 0.2	0	60-75	9.8 \pm 1.5, 22.6 \pm 1, 35.4 \pm 3
3	5.26 ± 0.6	-12.3	0	0	24-65	24.6 \pm 0.2 (~50)
This paper	5.68 ± 0.010 ± 0.05	-11.34 ± 0.11 ± 0.3	-3.55 ± 0.10 ± 0.3	0.21 ± 0.15 ± 0.3	20-150 (relative error) (systematic error)	22.32
This paper	Calculated ZFS (GHz): 8.07, 23.10, 31.17, 36.47, 59.57, 67.64					
This paper	Calculated zero-field energies (GHz); 23.17(A_{1u}), 15.10 (T_{1u}), -8.00(T_{2g}), -44.74(A_{1g})					

above 55 GHz. Finally, the points representing the lower satellite in Fig. 4 fall nicely between the transitions 1-5 and 2-6, i.e., close to the expected average.

The tunneling parameters giving the lowest rms relative error are listed in Table III which also includes, for comparison, the tunneling parameters, the dipole moment, and the ZFS available in the literature. Included also are the small relative rms errors and the large systematic errors, which clearly dominate the former. In the abstract we quote the combination of both sources of errors.

Summarizing, our new results, while more complete, are consistent with the earlier PER data. The only exception being the extrapolated ZFS located at ~50 GHz in Ref. 3. However, since it is based on broad and weak resonances it should be treated with caution. Hence we enclosed 50 GHz in parentheses in Table III.

In another type of investigation Wahl and Lüty¹⁷ estimated the size of the tunneling parameters from dielectric loss measurements as a function of electric field E . Their values for η ($\eta \approx 12$ GHz) and μ ($\mu \approx 4$ GHz)¹⁸ are quite consistent with our values but the results for ν are roughly an order of magnitude larger.

Their experiments clearly show that a finite value of ν exists but the actual value is difficult to extract from the data because of various broadening effects. For two of their experiments—one for which both μ and ν are present, and the other using an arrangement for which only ν is important—the width of the dips are essentially the same, but the depth of the dips are quite different. This suggests that ν is less than μ if one assumes the widths are determined by the electric field and/or stress broadening. Unfortunately, however, there is no way to obtain accurate values for μ and ν without knowing the stress

and electric field broadening components independently.¹⁸ In view of these considerations, the results obtained by Wahl and Lüty for ν are not in serious contradiction with our results.

V. DISCUSSION AND CONCLUSION

We have listed the existing data on PER in KCl:Li⁺ in Table II. It includes the estimated tunneling parameters, the microwave frequencies, the ZFS, and some additional data.

As can be seen, our estimate of the dipole moment is close to that in Refs. 1 and 3. These values are uncorrected for the Lorentz field. [The uncorrected dipole enters Eq. (4).] The corrected value is 2.43 \pm 0.03 D. The estimates of η in Refs. 1 and 2 are close to ours which is a surprise especially when one remembers that they were obtained from resonances lying at narrow frequency bands. The ν parameter is small but positive. However, the estimated error is large and this parameter may in fact be zero. One observation supporting equal energy spacings at $E=0$ made in Ref. 1 was that the line shapes at 23.1 GHz did not change on going from 4.2 to 1.7 K at $E=0$. The new parameters do not markedly change this: The transition probability at 23.1 GHz for the $T_{2g}-T_{1u}$ transition changes from 44% to 30% of the total—a change which would be hard to detect experimentally. However, as was discussed in Ref. 5, the estimates of μ and ν in Ref. 1 place a large upper bound on their values.

We have taken steps to minimize the accrued errors in locating the resonances by including as many of them in the numerical analysis as were available. As mentioned in Sec. IV, some 260 were included. The computer program described in Sec. IV evaluated the tunneling parameters so that the rms error between the experimental points and the calculated

resonances was minimized. The $\langle 111 \rangle$ model was most successful. We tried the $\langle 110 \rangle$ model also. It returned the parameters $p = 5.59$ D, $\eta = -12.64$, $\mu = -3.41$, $\nu = 2.35$, and $\sigma = 0.49$ (all in GHz). However, this model failed to account for the fact that many allowed resonances which the model predicted were not observed experimentally. We also tried to include an excited $\langle 111 \rangle$ multiplet in the program. The results obtained indicated no improvement in the rms error.

To conclude, our results based on the PER data gathered over a frequency range of 20–150 GHz support the $\langle 111 \rangle$ tunneling model of the ⁷Li⁺ center in KCl. They confirm the earlier analysis

done on this system. Additional tunneling parameters μ and ν were estimated. The parameter η and the electric dipole moment p were found to differ little from those available in the literature.

ACKNOWLEDGMENTS

One of us (F.H.) wishes to thank the Natural Sciences and Engineering Research Council of Canada for a travel grant and the University of Windsor, Ontario, Canada, for financial support in the form of a sabbatical leave. This work was supported in part by the National Science Foundation Grant No. DMR-78-1976.

-
- ¹R. A. Herendeen and R. H. Silsbee, *Phys. Rev.* **188**, 645 (1969).
- ²D. Blumenstock, R. Osswald, and M. C. Wolf, *Z. Phys.* **231**, 333 (1970).
- ³A. V. Frantsesson, D. F. Dudnik, and V. B. Kravchenko, *Fiz. Tverd. Tela (Leningrad)* **12**, 160 (1970) [*Sov. Phys.—Solid State* **12**, 126 (1970)].
- ⁴D. Blumenstock, R. Osswald, and M. C. Wolf, *Phys. Status Solidi B* **46**, 217 (1971).
- ⁵T. R. Larson and R. H. Silsbee, *Phys. Rev. B* **5**, 778 (1972).
- ⁶D. S. Channin, V. Narayanmuoti, and R. D. Pohl, *Phys. Rev. Lett.* **22**, 524 (1969).
- ⁷F. S. Vagapova and G. M. Ershov, *Fiz Tverd. Tela (Leningrad)* **22**, 392 (1979) [*Sov. Phys.—Solid State* **21**, 233 (1979)].
- ⁸T. R. Larson and R. H. Silsbee, *Phys. Rev. B* **6**, 3927 (1972).
- ⁹C. R. A. Catlow, K. M. Diller, M. J. Norgett, J. Cornish, and B. M. C. Parker, *Phys. Rev. B* **18**, 2739 (1978).
- ¹⁰M. J. L. Sangster, *J. Phys. C* **13**, 5279 (1980).
- ¹¹F. Bridges, *Crit. Rev. Solid State Sci.* **5**, 1 (1975).
- ¹²F. Bridges, *Rev. Sci. Instrum.* **45**, 130 (1974).
- ¹³F. Holuj and F. Bridges, *Phys. Rev. B* **20**, 3578 (1979).
- ¹⁴*Handbook of Chemistry and Physics*, edited by Robert C. Weast (Chemical Rubber, Cleveland, 1979).
- ¹⁵C. A. Harper, *Handbook of Materials and Processes for Electronics* (McGraw-Hill, New York, 1970).
- ¹⁶B. Fox, F. Holuj, and W. E. Baylis, *J. Magn. Reson.* **10**, 347 (1973).
- ¹⁷J. Wahl and F. Lüty, *Ferroelectrics* **17**, 371 (1977).
- ¹⁸F. Lüty (private communication).